Nonlinear state and parameter estimation for a Gas-Liquid Cylindrical Cyclone

Torstein Thode Kristoffersen* and Christian Holden*

***Abstract*— New offshore oil and gas discoveries are located at deep waters with long tie-back distances. Development of such fields require compact gas-liquid separation technologies. Efficient operation of such separators require multiple sensors and advanced controllers. However, the number of available sensors at the seabed is often limited due to low reliability (failures and low sampling frequency), lack of suitable sensor technology and/or high cost. Therefore, this paper develops a nonlinear MHE and UKF for estimation of indirectly measured and unmeasured variables. The estimates are used as state feedback to a linear MPC to study their estimation performance in simulations.**

I. INTRODUCTION

Most of the mature offshore oil and gas discoveries are exhausted and new offshore oil and gas discoveries are located in deep waters with longer tie-back distances. Subsea processing is an enabling technology for the development of these new fields and for increased oil and gas recovery of mature fields. Subsea gas-liquid separation is a key component of subsea processing for several reasons, including (i) a reduced number of flowlines and topside processing capacity, (ii) cost efficient hydrate management, (iii) single-phase boosting required to overcome high static pressure at deep waters and (iv) enabling longer range gas compression from subsea to onshore processing facility [1].

The Gas-Liquid Cylindrical Cyclone (GLCC) separator is a compact centrifugal-based separator suited for subsea separation. A sketch of the separator is shown in Fig. 1. This separator is preferred for subsea applications over large gravity-based separator due to its simple and compact construction that allow for installation at deep waters and remote operation requiring little maintenance [2]. The performance of the separator depends on several variables and therefore, multiple sensors are required to achieve efficient operation [3].

A major challenge with subsea processing is that the equipment is located on the seabed and is not easily available for maintenance. Maintenance interventions require good weather conditions and specialized lifting vessels that are costly and need to be hired several months in advance. Therefore, sensors must be robust and reliable to withstand the harsh environment on the seabed and operate without failures for very long periods. However, sensors are prone to failures, and the sensor data quality is often low due to indirect sensing and/or too low sampling frequency of a process variable. Additionally, and especially for subsea processing, the number of sensors are often limited due to too expensive sensors and/or lack of suitable sensor technology [4].

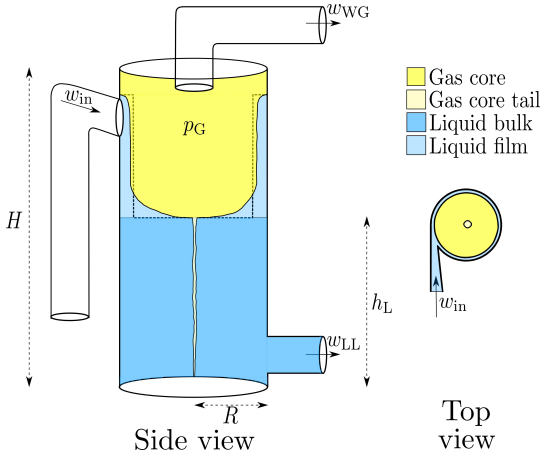

Fig. 1. A sketch of a gas-liquid cylindrical cyclone separator showing the separator volumes, the pressure and liquid level and the inlet and outlet flows. The actual parabolic gas-liquid interface and the approximated gas-liquid interface are illustrated by solid and dashed lines, respectively.

Estimators, or soft sensors, are a cost-efficient alternative to physical sensors, using a mathematical model of the plant and available measurements to filter measured states and estimate unmeasured states and parameters. Estimators are categorized either as stochastic or deterministic estimators based on whether the estimates are modelled as stochastic or deterministic variables. The Kalman Filter (KF) is an optimal stochastic estimator for estimation of linear systems [5]. The estimation of nonlinear systems is a challenging problem and several extensions of the KF has been developed, including the Extended Kalman Filter (EKF) and the Unscented Kalman Filter (UKF) [6]. The Moving Horizon Estimator (MHE) is a deterministic optimization-based method for estimation of linear or nonlinear systems. The method applies a linear model of the plant and finds the best estimates that fits past measurements on a finite moving time window. The Nonlinear MHE (NMHE) is an extension of the MHE for estimation of nonlinear systems using a nonlinear model. The main advantage of the NMHE is the explicit consideration of nonlinear systems and constraints, but also the optimality of the estimates and proven stability properties [7].

The GLCC separator has been subject to extensive studies on control and an overview is provided in [8]. The proposed controllers typically achieve efficient control of the separator, but require knowledge of several process variables and parameters. Estimation of states and parameters for the GLCC separator has received less attention in the literature.

* Department of Mechanical and Industrial Engineering, Norwegian University of Science and Technology (NTNU). torstein.t.k@gmail.com, christian.holden@ntnu.no

In [9], the feedback linearizing controller proposed in [10] was extended with adaptation of the unknown states and parameters. In [8], a Model Predictive Controller (MPC) using state feedback from an EKF was proposed, but the EKF gave low robustness and assumed knowledge of two unmeasured states. Therefore, [11] investigated the performance of an UKF and a linear MHE using a nonlinear measurement model based on measured states. However, although the linear MHE achieved good estimates of the directly and indirectly measured states, it was only able of accurately predicting one of the two unknown parameters. Additionally, the UKF used for comparison operated at significantly higher frequency than that of the MHE.

In this paper, we derive an NMHE to achieve improved accuracy of the unknown parameters and extend the UKF based on [11] so that both operate at the same frequencies equal to that of the sensors providing measurements. The simplified estimation model derived in [11], consisting of four states (two directly and two indirectly measured) and two unknown parameters, is applied by both estimators. The measurements are inverted prior to running the estimators to have a linear relationship between the estimates and measurements. The estimators are specially designed to compensate for the fast sampling of the states and the relatively slow sampling of the measurements. The estimates calculated by the estimators are used as state feedback for the MPC developed in [8] to study their estimation performance in simulations.

II. DYNAMIC MODEL

The GLCC separator is constructed as a vertical tank as shown in Fig. 1. The gas-liquid inlet flow w_{in} enters tangentially through a downward inclined inlet resulting in a rotational motion of the fluid inside the separator. The rotational motion of the fluid creates high centrifugal forces that separates the gas from the liquid due to their density difference. The separated liquid falls down to the bottom and establishes a liquid level h_{L}, while the separated gas rises to the top and establishes a gas pressure p_{G}. The residence time of the fluid inside the separator is short resulting in incomplete separation of the gas-liquid inlet flow. The gas leaving through the upper outlet w_{WG} will contain some droplets and is therefore called Wet Gas (WG), while the liquid leaving through lower outlet w_{LL} will contain some gas bubbles and is therefore called Light Liquid (LL). The LL and WG are the two main volumes inside the separator.

A dynamic model describing the initial separation was first presented in [12] and later extended in [13] to include continuous separation. In this paper, we use the latter model given by

$$\begin{aligned}\dot{m}_{\text{LL,L}} = &(1-\beta_{\text{in}})w_{\text{in}} - \epsilon_{\text{in,L}}(1-\beta_{\text{in}})w_{\text{in}} \\ &+ \epsilon_{\text{L}}(1-\beta_{\text{WG}})m_{\text{WG,L}} - (1-\beta_{\text{LL}})w_{\text{LL}}\end{aligned} \tag{1}$$

$$\dot{m}_{\text{LL,G}} = \epsilon_{\text{in,G}}\beta_{\text{in}}w_{\text{in}} - \epsilon_{\text{G}}\beta_{\text{LL}}m_{\text{LL,G}} - \beta_{\text{LL}}w_{\text{LL}} \tag{2}$$

$$\begin{aligned}\dot{m}_{\text{WG,L}} = &\epsilon_{\text{in,L}}(1-\beta_{\text{in}})w_{\text{in}} - \epsilon_{\text{L}}(1-\beta_{\text{WG}})m_{\text{WG,L}} \\ &- (1-\beta_{\text{WG}})w_{\text{WG}}\end{aligned} \tag{3}$$

$$\dot{m}_{\text{WG,G}} = \beta_{\text{in}}w_{\text{in}} - \epsilon_{\text{in,G}}\beta_{\text{in}}w_{\text{in}} + \epsilon_{\text{G}}\beta_{\text{LL}}m_{\text{LL,G}} - \beta_{\text{WG}}w_{\text{WG}}, \tag{4}$$

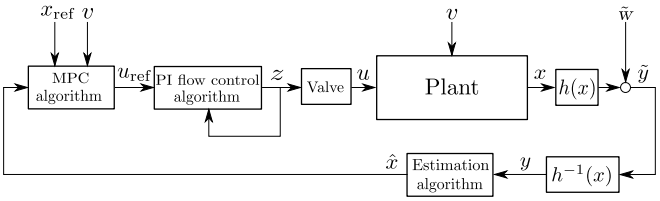

Fig. 2. A block diagram of the closed-loop system.

where the state $m_{\text{x,y}}$ is the mass of component y in x, $\beta_{\text{in}} \in [0,1]$ is the inlet gas mass fraction, $\beta_{\text{x}} \in [0,1]$ is the gas mass fraction in x, $\epsilon_{\text{in,y}} \in [0,1]$ is the immediate separation of component y at the inlet and $\epsilon_{\text{y}} \in [0,1]$ is the continuous separation of component y. The subscript x represents either in (inlet), WG or LL and the subscript y represents either G (gas) or L (liquid).

The model includes four algebraic state equations: two for describing the gas mass fraction in each of the main volumes, i.e., β_{LL} and β_{WG}; and two for describing the controlled variables, i.e., the level h_{L} and pressure p_{G}. The algebraic states are given by

$$\beta_{\text{LL}} = \frac{m_{\text{LL,G}}}{m_{\text{LL,L}} + m_{\text{LL,G}}} \tag{5}$$

$$\beta_{\text{WG}} = \frac{m_{\text{WG,G}}}{m_{\text{WG,L}} + m_{\text{WG,G}}} \tag{6}$$

$$h_{\text{L}} = \frac{m_{\text{LL,L}} + m_{\text{LL,G}}}{a} \tag{7}$$

$$p_{\text{G}} = \frac{bm_{\text{WG,G}}}{aH - (m_{\text{LL,L}} + m_{\text{LL,G}})}, \tag{8}$$

where H is the total tank height and a and b are constants.

A control valve is mounted on both outlets and the outlet flows are determined by the respective control valve opening percentage $z = [z_{\text{WG}}, z_{\text{LL}}]^\top$. A PI flow controller calculates the opening percentage for the respective outlet flow based on a flow reference generated by the MPC. These two flow references are the manipulated variables for the control system.

III. CONTROL DESIGN

The plant is controlled by an output MPC in cascade with two PI flow controllers as shown by the block diagram in Fig. 2. The applied output MPC uses state feedback from an estimator to control the level and pressure by calculating the flow references $u_{\text{ref}} = [u_{\text{LL,ref}}, u_{\text{WG,ref}}]^\top$ to the PI flow controllers. The MPC was derived in [8] and the following summary is only included for completeness.

The optimal control objective for the MPC is to track the level and pressure references without excessive changes in control inputs. The MPC achieves optimal control by, at each discrete time step k, solving a discrete-time Optimal Control Problem (OCP) over a prediction horizon T_h. The first vector element of the optimal control input sequence is applied to the plant and the process is repeated at the next discrete time step $k+1$. This procedure is known as the MPC principle [14].

The OCP is structured as a Quadratic Programming (QP) problem specified by a objective function J_{MPC} weighting

deviations in states and inputs from desired references x_{ref} and u_{ref}, respectively, subject to constraints enforcing the dynamics and limiting the feasible states and inputs values. To have a convex OCP with respect to the state and control input variables (decision variables), the MPC uses a transformed state-space model of (1)–(4) to predict the future behaviour of the system. The mapping is given by

$$x = T(m) = [h_{\text{L}}, p_{\text{G}}, m_{\text{LL,G}}, m_{\text{WG,L}}]^\top, \tag{9}$$

where x is the transformed state vector.

The MPC uses a different sampling rate of the states and control inputs to have fast enough sampling of the states to capture the fast dynamics of the plant (1)–(4) and a slow enough sampling of the control inputs to adapt for industrial applications. The OCP solved by the MPC is given by

$$\begin{aligned}\min_{u_{\text{ref}}} J_{\text{MPC}} = &\sum_{i=0}^{N} \frac{1}{||x_{\text{ref}}||_2^2} \big|\big|x_i - x_{\text{ref},i}\big|\big|_Q^2 \\ &+ \sum_{i=0}^{N_u} \frac{1}{||u_{\infty,i}||_2^2} \big|\big|u_i - u_{\infty,i}\big|\big|_R^2 \end{aligned} \tag{10}$$

$$\text{s.t.} \quad x_0 = x_k \tag{11}$$

$$x_{\min} \le x_i \le x_{\max} \;\; \forall\, i \in \{0, \dots, N\} \tag{12}$$

$$u_{\min} \le u_i \le u_{\max} \;\; \forall\, i \in \{0, \dots, N_u\}, \tag{13}$$

where $Q \ge 0$ is the diagonal state weighting matrix, $R \ge 0$ is the diagonal control weighting matrix, $N = T_h/\Delta t_s$ is the state samples over T_h where Δt_s is the sampling time of the states, $N_u = T_h/T_u$ is the number of control input samples over T_h where Δt_u is the sampling time of the control inputs and the subscript max and min denotes upper and lower bounds. The notation $||z||_M^2 = z^\top M z$ is used in this paper.

IV. ESTIMATOR DESIGN

The plant states are estimated by a nonlinear estimator providing state feedback to the MPC. The estimators are based on the same transformed state-space model as the MPC and uses the available measurements of the inlet conditions w_{in} and β_{in}, the level h_{L}, the pressure p_{G} and the two outlet gas mass fractions β_{LL} and β_{WG} to estimate the transformed states x. The estimation model was derived in [11] and is included in this section for completeness.

A. Estimation Objective

The estimation objective is to calculate approximate values of the states and parameters, with minimum error mean (bias) and variance, for the MPC to control the plant.

B. Estimation Model

The estimators use the same transformed state-space model (9) as the MPC, consisting of four states and four separation factors. However, only four measurements are available at the plant output resulting in limited system observability. Therefore, to enable estimation of the system states, the transformed state-space model is augmented with two additional states and simplified by collecting the separation factors into two unknown parameters. The augmented, transformed state-space model is given by

$$\dot{x}_1 = \frac{1}{a}\big[v_1 - \theta_1 + \theta_2 - w_{\text{LL}}\big] + w_1 \tag{14}$$

$$\begin{aligned}\dot{x}_2 = \frac{c_2}{a(H-x_1)}\Big[b\Big(v_2 - \theta_2 - \frac{a(x_2/c_2)(H-x_1)}{bx_4 + a(x_2/c_2)(H-x_1)} w_{\text{WG}} \\ + \Big(\frac{x_2}{c_2}\Big)\Big(v_1 - \theta_1 + \theta_2 - w_{\text{LL}}\Big)\Big] + w_2\end{aligned} \tag{15}$$

$$\dot{x}_3 = \theta_2 - \frac{x_3}{ax_1} w_{\text{LL}} + w_3 \tag{16}$$

$$\dot{x}_4 = \theta_1 - \frac{a(x_2/c_2)(H-x_1)}{bx_4 + a(x_2/c_2)(H-x_1)} w_{\text{WG}} + \text{w}_4 \tag{17}$$

$$\dot{\theta}_1 = w_5 \tag{18}$$

$$\dot{\theta}_2 = w_6, \tag{19}$$

where $w = [w_1, w_2, w_3, w_4, w_5, w_6]^\top \sim \mathcal{N}(0, W)$ is white process noise with covariance W disturbing the states, $v = [v_1, v_2]^\top = [(1-\beta_{\text{in}})w_{\text{in}}, \beta_{\text{in}} w_{\text{in}}]^\top$ is inlet flow and $\theta = [\theta_1, \theta_2]^\top$ is the unknown time-varying parameters. The variable x_2 is scaled from Pa to bar using the scaling variable $c_2 = 10^{-5}$.

The available measurements give the following observation model

$$\tilde{y} = \Big[x_1, x_2, \tfrac{x_3}{ax_1}, \tfrac{ax_2(H-x_1)}{ax_2(H-x_1)+bx_4}, 0, 0\Big]^\top + \tilde{\text{v}}, \tag{20}$$

where $\tilde{v} = [\tilde{v}_1, \tilde{v}_2, \tilde{v}_3, \tilde{v}_4, \tilde{v}_5, \tilde{v}_6]^\top \sim \mathcal{N}(0, \tilde{V})$ is white measurement noise with covariance $\tilde{V}$ disturbing the measurements and $\tilde{y}$ is the measurements.

A compact description of the estimation model is given by

$$\dot{\tilde{x}} = f(\tilde{x}(t), \tilde{u}(t)) + w \tag{21}$$

$$\tilde{y} = h(\tilde{x}(t)) + \tilde{\text{v}}, \tag{22}$$

where $\tilde{x} = [x, \theta]^\top$ is the augmented state vector, $\tilde{u} = [w, v]^\top$ is the augmented inputs, $f(\cdot)$ is the nonlinear prediction function comprising (14)–(19) and $h(\cdot)$ is the nonlinear observation function given by (20).

To get a linear relationship between the measurements and the augmented states, the nonlinear observation model (22) is inverted yielding

$$y = h^{-1}(\tilde{y}) = h^{-1}(h(\tilde{x} + \tilde{v})) \approx h^{-1}(h(\tilde{x})) + v = \tilde{x} + v, \tag{23}$$

where y is an approximation of the inverted measurements and $v = [v_1, v_2, v_3, v_4, v_5, v_6]^\top \sim \mathcal{N}(0, V)$ with white measurement noise and constant covariance V.

C. Implementation and Discretization

The plant, controller and estimators are implemented in MATLAB using CasADi version 3.1.0. CasADi is a software for numerical optimal control and algebraic differentiation [15]. The continuous-time nonlinear estimation model (21)–(22) is implemented symbolically using CasADi and discretized using the numerical integrator CVODES [16] with sampling Δt_s equal to that of the simulation. The discrete-time nonlinear estimation model is given by

$$\tilde{x}_{k+1} = \tilde{f}(\tilde{x}_k, \tilde{u}_k) + w_k \tag{24}$$

$$y_k = \tilde{x}_k + v_k, \tag{25}$$

where $\tilde{f}(\tilde{x}_k, \tilde{u}_k)$ is the discrete-time nonlinear prediction model, $w_k \sim \mathcal{N}(0, W\Delta t_s)$, $v_k \sim \mathcal{N}(0, V\Delta t_s)$ and k is the time step. The symbolic expressions are calculated offline and evaluated numerically online by substituting symbolic variables for numerical values. The interior-point solver IPOPT [17] is used to solve the optimization problems generated by the MPC and NMHE. CVODES and IPOPT are external software interfaced through CasADi.

D. Unscented Kalman Filter

The discrete-time UKF is a stochastic nonlinear state estimator that estimates the augmented states $\tilde{x}_k$ at discrete time steps in two estimation steps: first by a *prediction step* and subsequently by a *correction step*. The estimates are modelled as a random variable described by its mean $\hat{x}_k$ and error covariance P_k. The prediction step time propagates the *a posteriori* estimate $\hat{x}^+_{k-1}$ and P^+_{k-1} from the previous time step using the discrete-time prediction model (24) to obtain the current time step *a priori* estimate $\hat{x}^-_k$ and P^-_k. The correction step corrects the current time step a priori estimate for the recent measurement $\tilde{y}_k$ using the discrete-time observation model (25) and the Kalman gain K_k to obtain the current time a posteriori estimate. The mean state estimate $\hat{x}_k = \hat{x}^+_k$ is provided as state feedback to the MPC.

The frequency of the UKF is changed from that used in [11] to that of the NMHE to operate the UKF at the same frequency as the MPC and the sensors providing measurements, i.e., changed from executing each Δt_s second to each Δt_y second where Δt_y is the sampling time of the observations. This also enables a fairer comparison between the UKF and NMHE. The sampling frequency of the system dynamics are much faster than the sampling frequency of the measurements. Therefore, before each measurement update, the estimators need to integrate the previous time a posteriori estimate, over a time step equal to the sampling time of the measurements, to obtain the current time a priori estimate.

The UKF is based on the principle that an approximation of the random variable properties based on a set of transformed points, called *sigma points*, is more correct than an estimate of the random variable properties based on a single point [6]. This approximation achieves provably increased accuracy of the estimates $\hat{x}_k$ and P_k compared to the EKF at the expense of increased computational cost [6]. Two sets of sigma points are chosen for each of the estimation steps. The sigma points for the prediction step $\mathcal{X}_{k-1}$ are chosen based on $\hat{x}^-_{k-1}$ and P^-_{k-1}, while the sigma points for the correction step $\mathcal{X}_k$ are based on $\hat{x}^+_k$ and P^+_k. The mean and error covariance for each of the estimation steps are approximated as the sample mean of the transformed sigma points using the corresponding model for the estimation step. The sigma points are chosen according to the distribution

$$\mathcal{X}_{i,k} = \begin{cases} \hat{x}^\star_k + \left(\sqrt{nP^\star_k}\right)_i & \forall\, i = 1, \ldots, n \\ \hat{x}^\star_k - \left(\sqrt{nP^\star_k}\right)_i & \forall\, i = 1+n, \ldots, 2n\,, \end{cases} \tag{26}$$

where $\mathcal{X}_{i,k}$ is ith sigma points at time k in the set of sigma points $\mathcal{X}_k$, n is the dimension of $\hat{x}_k$, $\sqrt{nP^\star_k}_i$ is the ith row of $\sqrt{nP^\star_k}$ and $\star$ represents either a priori estimate $(-)$ or a posteriori estimate $(+)$.

Algorithm 1 Discrete-time UKF

Require: Input: $\tilde{y}_k$, $\hat{x}_{k-1}$, $\tilde{u}_{k-1}$, P^+_{k-1}, W, V

if mod(time, Δt_y) == 0 **then**
  PREDICTION STEP
  for $j = 1$ to $\Delta t_y / \Delta t_s$ **do**
    Choose $\mathcal{X}_{k-1}$ by (26) using $\hat{x}^+_{k-1}$ and P^+_{k-1}
    Calculate $\mathcal{X}_{i,k} = \tilde{f}(\mathcal{X}_{i,k-1}, \tilde{u}_{k-1})$
    Update $\hat{x}^-_k = \frac{1}{2n}\sum_{i=1}^{2n} \mathcal{X}_{i,k}$
    Update $P^-_k = \frac{1}{2n}\sum_{i=1}^{2n} ||\mathcal{X}_{i,k} - \hat{x}^-_k||^2 + W$
  CORRECTION STEP
  Choose $\mathcal{X}_k$ according to (26) using $\hat{x}^-_k$ and P^-_k
  Calculate $\mathcal{Y}_{i,k} = \mathcal{X}_{i,k}$
  Update $\hat{y}_k = \frac{1}{2n}\sum_{i=1}^{2n} \mathcal{Y}_{i,k}$
  Calculate K_k using $\mathcal{X}_k$, $\hat{x}^-_k$, $\mathcal{Y}_k$, $\hat{y}_k$ and V
  Update $\hat{x}^+_k = \hat{x}^-_k + K_k(\tilde{y}_k - \hat{y}_k)$
  Update $P^+_k = P^-_k - K_k\left(\frac{1}{2n}\sum_{i=1}^{2n} ||\mathcal{Y}_{i,k} - \hat{y}_k||^2 + V\right)^{-1} K_k^\top$
  return $\hat{x}_k = \hat{x}^+_k$ and $P_k = P^+_k$
else
  return $\hat{x}_k = \hat{x}_{k-1}$ and $P_k = P^+_{k-1}$

The pseudo code of the implemented discrete-time UKF is given in Algorithm 1 and is based on [18] and [19, Ch. 14].

E. Nonlinear Moving Horizon Estimation

The NMHE is a deterministic, optimization-based state observer that estimates the augmented states $\tilde{x}_k$ at discrete time steps. The estimates are modelled as deterministic variables. The estimate at a discrete-time step is calculated by solving an Optimal Estimation Problem (OEP) using N previous observations of the measurements and inputs on a fixed-size moving time window to obtain a posteriori sequence of state estimates $\hat{X}_k = \hat{X}^+_k$ that best fits these observations. The observations at time step k on the moving time window is gathered in the information vector ι_k.

The OEP is structured as a Nonlinear Programming (NLP) problem with a objective function J_{MHE} weighting deviations between the estimated states $\tilde{x}$ from the past observations subject to constraints enforcing the discrete-time estimation model and limiting the feasible estimated states. The last vector element of the optimal state estimation sequence $\tilde{x}_k$ is provided as state feedback to the MPC.

The NMHE executes at discrete time instants when new measurements are available, i.e., each Δt_y second. New measurements are added to the moving time window and the oldest are removed at the beginning of each execution. Similar to the UKF, the fast sampling of the states relative to the slow sampling of the measurements requires the NMHE to operate with different sampling of the states and observations. Thus, the information vector is given by

$$\iota_k = [y_{k-N+N_x}, \ldots, y_{k-N+N_y N_x}, \tilde{u}_{k-N}, \ldots, \tilde{u}_{k-N+N_y N_x}], \tag{27}$$

where $N = T_h/\Delta t_s$ is the moving window horizon, T_h is the time horizon of the moving window, $N_y = T_h/\Delta t_y$ is the number of gathered observations and $N_x = N/N_y = \Delta t_y/\Delta t_s$ is the number of states predictions between each observation sample.

The OEP only considers the N most recent observations, as observations further into the past are removed from the moving time window as new observations are added. The NMHE approximates the importance of these discarded observations by including a weighting term in the objective function called the *arrival cost* and requiring knowledge of the a posteriori estimate $\hat{x}_{k-N} = \hat{x}^+_{k-N}$. The OEP solved by the NMHE at each discrete-time step is given by

$$\min_{\tilde{x},\mathrm{v},\mathrm{w}} J_{\mathrm{MHE}} = \left|\left|\hat{x}_{k-N} - \tilde{x}_{k-N}\right|\right|^2_{S^{-1}} + \sum_{i=1}^{N_y} \left|\left| v_{k-N+iN_x} \right|\right|^2_{V^{-1}} + \sum_{i=1}^{N_y} \sum_{j=0}^{N_x-1} \left|\left| w_{k-N+(i-1)N_x+j} \right|\right|^2_{W^{-1}} \tag{28}$$

$$\text{s.t.} \quad \hat{x}_{k-N} = \tilde{f}(\tilde{x}_{k-N-1-N_x}, \tilde{u}_{k-N-1-N_x}) \tag{29}$$

$$\tilde{x}_{k-N+1+i} = f_k(\tilde{x}_{k-N+i}, \tilde{u}_{k-N+jN_x}) + w_{k-N+i} \quad \forall\, i \in \{k-N, \dots N-1\},\ j \in \{1, \dots N_y\} \tag{30}$$

$$y_{k-N+iN_x} = \tilde{x}_{k-N+iN_x} + v_{k-N+iN_x} \quad \forall\, i \in \{1, \dots N_y\} \tag{31}$$

$$x_{\min} \leq \tilde{x}_i \leq x_{\max} \quad \forall\, i \in \{k-N, \dots N\}, \tag{32}$$

where $W \geq 0$ is the diagonal state prediction weighting matrix expressing the confidence in the state prediction, $V \geq$ is the diagonal predicted observation weighting matrix expressing the confidence in the past measurements, and $S \geq 0$ is the diagonal arrival cost weighting matrix indicating the importance of the discarded information that is not part of the moving time window.

The OEP is simplified by substituting the equality constraints into the objective function and transcribed using the multiple shooting method. In order to ensure a feasible starting point for the numerical solver and reduce the computational time required to solve the OEP, the NMHE is provided with an initial guess of the estimates $\hat{X}^-_k = [\hat{x}^-_{k-N}, \dots, \hat{x}^-_k]^\top$. The initial guess is the a priori estimates for the NMHE computed by time shifting the previous a posteriori estimates one time step into the future. The empty data space for current time a priori estimate is padded with the previous time a posteriori estimate.

The pseudo code of the implemented NMHE is given in Algorithm 2 and is based on [7], [20].

F. Tuning

The quality of the estimates depends on the tuning of the weighting matrices. Ideally, for the case without plant-model-mismatch, W and V would equal the process and measurement variance noise, respectively. However, this is rarely the case and tuning of these matrices are necessary to achieve good estimation performance. Therefore, these matrices were tuned by trial-and-error until satisfactory performance was achieved. Good tuning gives less noisy estimates as well as faster convergence to the true states, but does not remove deviations between an estimate and the true value.

TABLE I

STATISTICAL NOISE PROPERTIES.

A_z[%]	$\mu_{w_{\text{in}}}$[kg/s]	$\mu_{\beta_{\text{in}}}$[-]	$\mu_{h_{\text{L}}}$[m]	$\mu_{p_{\text{G}}}$[bar]	$\mu_{\beta_{\text{LL}}}$[-]	$\mu_{\beta_{\text{WG}}}$[-]
3.00	12.40	0.23	1.50	50.00	0.05	0.85

Algorithm 2 NMHE

Require: Input: $\hat{x}_{k-N-1-N_x}, \tilde{u}_{k-N-1-N_x}, \iota_k, \hat{X}_{k-1}, S, W, V$

```
if mod(time, Δt_y) == 0 then
    Update X̂_k^- by time shifting X̂_{k-1}^+
    Substitute inputs for symbolic variables
    Update and solve NLP (28)–(32) to obtain x̂_k^+ = x̃_k
    return x̂_k = x̂_k^+
else
    return x̂_{k-1}
```

V. SIMULATIONS AND DISCUSSION

The performance of the estimators were studied in separate simulations, shown in Figs. 3–4, for changing inlet conditions using measurements with additive band-limited zero-mean Gaussian white noise. The noise variance is given by $\sigma_z = (A_z \mu_z)^2$ where σ_z is the standard deviations of measurement z, A_z is the variation of z and μ_z is the mean nominal value of z. The mean nominal values are determined a priori of the simulations and are given in Table I. The inlet conditions changed between a low, intermediate and high inlet gas mass fraction flow using physical properties and parameters of 25° API crude oil at 50 bar and 30°C similar to [8]. The tuning and configuration parameters for the estimator that are used in the simulations are listed in Table II.

A general observation of the estimator performances in Figs. 3–4 show that both estimators achieve good estimation performance of the controlled variables, but indicate that the UKF achieves slightly better estimates for the indirectly measured states ($m_{\text{LL,G}}$ and $m_{\text{WG,L}}$) and the unknown parameters. However, the figures indicate that the differences between the estimators are small, and therefore the statistical properties of the estimation error $e = \hat{x} - \tilde{x}$ of all estimates, for both estimators, are calculated to objectively evaluate their per-

TABLE II

TUNING AND CONFIGURATION PARAMETERS.

Parameters	Value	Unit
Q	$\text{diag}[8000; 8000; 0; 0; 1000; 1000]^\top$	-
R	$\text{diag}[200; 200]^\top$	-
T_h	15	s
Δt_u	1	s
Δt_y	1	s
Δt_s	0.02	s
W_{UKF}	$\text{diag}[0.001, 0.05, 0.001, 0.01, 0.01, 0.001]^\top$	-
V_{UKF}	$\text{diag}[0.001, 0.001, 0.1, 0.1]^\top$	-
$S_{\text{l-MHE}}$	$\text{diag}[1, 10^{-3}, 1, 10^{-3}, 10^{-8}, 10^{-8}]^\top$	-
$W_{\text{l-MHE}}$	$\text{diag}[0.001, 0.05, 0.001, 0.01, 0.0001, 0.00001]^\top$	-
$V_{\text{l-MHE}}$	$\text{diag}[0.001, 0.001, 0.1, 0.1]^\top$	-
$x_{\min}$	$[h_{\text{L,min}}, p_{\text{G,min}}, -\infty, -\infty, -\infty, -\infty]^\top$	-
$x_{\max}$	$[h_{\text{L,max}}, p_{\text{G,max}}, \infty, \infty, \infty, \infty]^\top$	-

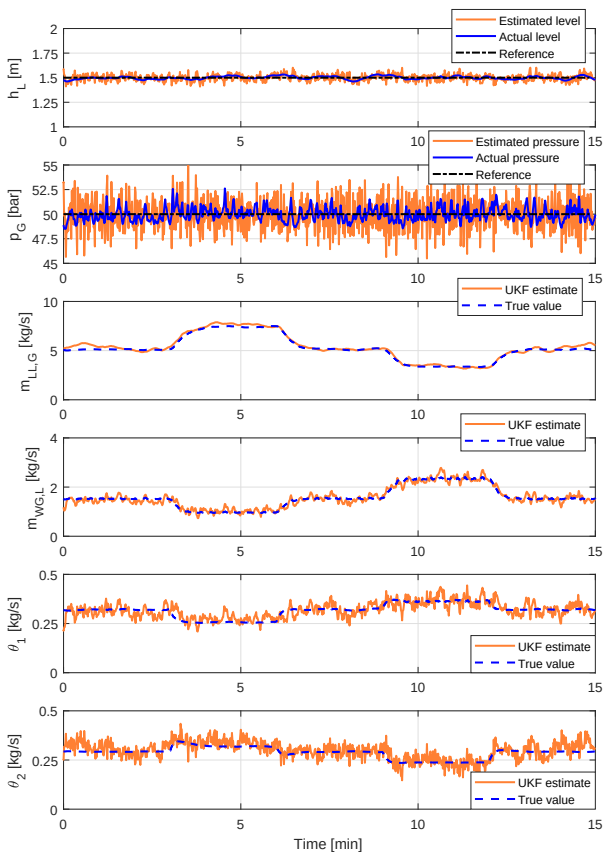

Fig. 3. Estimation performance of the discrete-time UKF.

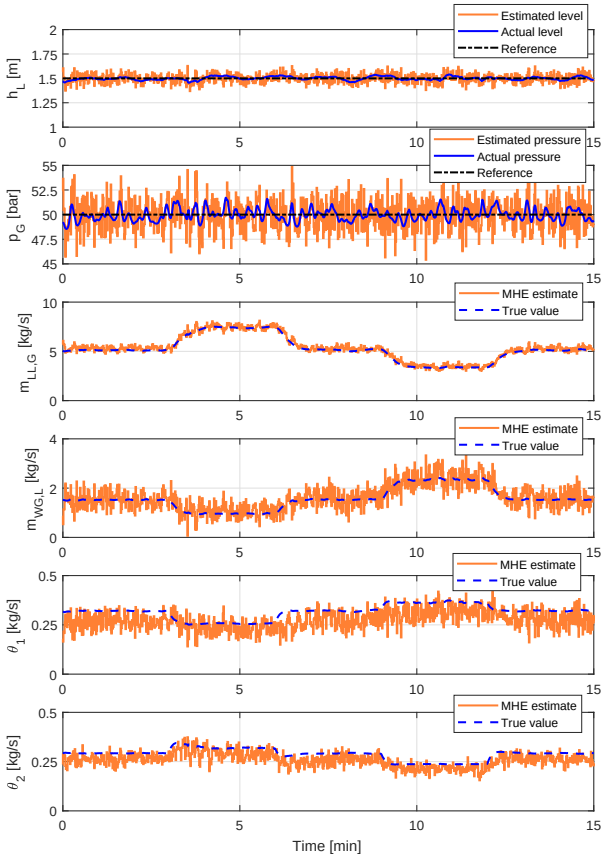

Fig. 4. Estimation performance of the discrete-time NMHE.

formances. As mentioned earlier, the estimator objective is to calculate unbiased estimates with minimum variance that satisfy constraints, i.e., $\mathrm{E}[e] = 0$ and $\min_e \mathrm{E}\big[(e - E[e])^2\big]$. The statistical properties are given in Table III.

The statistical properties show that the UKF achieves more accurate estimates than the NMHE with few exceptions and that the magnitudes are small. The UKF achieves a good estimate of h_L with negligible bias and variance and an acceptable estimate of p_G with small bias and reduced variance compared to the measurement noise. The NMHE achieves an equally good estimate of h_L and a better estimate of p_G with smaller bias and variance than the UKF. The UKF obtains good estimate of both $m_\mathrm{LL,G}$ and $m_\mathrm{WG,L}$ with small bias and reduced variance compared to the measurement noise. The NMHE achieves a good estimate of $m_\mathrm{LL,G}$, but only an acceptable estimate of $m_\mathrm{WG,G}$ with small bias and significant variance. The UKF achieves good estimates of both the unknown parameters θ_1 and θ_2 with negligible bias and small variance. The NMHE achieves tolerable estimates of θ_1 and θ_2. The bias of these estimates are larger than for the UKF, but with equally small variance.

TABLE III

STATISTICAL PROPERTIES FOR THE ESTIMATOR ERRORS.

Statistical properties	Mean $(\bar{e} = E[e])$ UKF	NMHE	Variance $(\sigma_e^2 = E[(e-\bar{e})^2])$ UKF	NMHE
h_L	−0.0005	−0.0013	0.0009	0.0015
p_G	−0.1043	−0.0606	2.1377	1.8136
$m_\mathrm{LL,G}$	0.1951	0.1077	0.0660	0.0453
$m_\mathrm{WG,L}$	−0.0086	0.0576	0.0119	0.0921
θ_1	−0.0004	−0.0408	0.0007	0.0015
θ_2	0.0098	−0.0370	0.0009	0.0007

A general observation of the controlled variables show acceptable control performance for the changes in inlet conditions with respect to the experimental start-up response in [3]. RMS values of the control error $e_\mathrm{ctrl} = \hat{x} - \tilde{x}_\mathrm{ref}$ and closed-loop system error $e_\mathrm{sys} = \tilde{x} - \tilde{x}_\mathrm{ref}$ are given in Table IV to enable objective evaluation of their performance. The RMS values measuring the control performance shows as expected that the MPC using state feedback from the UKF achieves slightly better level control, but poorer pressure control, than the MPC using state feedback from the NMHE. The same behaviour for the estimator performance is recognised by RMS values measuring the closed-loop system performance.

The slightly better overall estimation performance achieved by the UKF over the NMHE is not unexpected. Stochastic estimators like the UKF are designed to maximize the probability that the estimate is correct, given all the past measurements that are parametrized in the mean and

TABLE IV

RMS VALUES FOR THE CONTROL AND CLOSED-LOOP SYSTEM ERRORS.

RMS value	Control $(\hat{x} - \tilde{x}_\mathrm{ref})$ UKF	NMHE	System $(\tilde{x} - \tilde{x}_\mathrm{ref})$ UKF	NMHE
h_L	0.0359	0.0471	0.0171	0.0191
p_G	1.6425	1.6473	0.7543	0.6884

covariance, while deterministic estimators like the NMHE is designed to obtain the state trajectory that best fits a limited sequence of past measurements.

The dynamics of the a priori nonlinear prediction model (21) is largely described by the unknown parameters. This reduces the quality of the prediction model and causes significant errors in the state prediction.

A comparison of the performance of the UKF in this paper to that in [11] reveals that the oscillations are significantly increased. This increase is due to the increased sampling time between correction step resulting in an increased prediction step from Δt_s to Δt_y. However, the significant oscillations in p_{G} and the smaller oscillations in $m_{\mathrm{WG,L}}$ are likely to occur due to the relatively poor prediction model.

As expected, a comparison of the NMHE in this paper to that of the MHE in [11] with equal covariance matrices reveals that the NMHE generally achieves better estimates than the MHE, especially of θ_1 which was inaccurately estimated by the MHE with a large bias. The significant oscillations in p_{G} is likely to caused by the relatively poor prediction model.

VI. CONCLUSIONS AND FURTHER WORK

This paper presents a nonlinear UKF and MHE with different frequencies for state prediction and measurements update for the estimation of unmeasured states and parameters of a GLCC separator. These estimators provide state feedback to an output MPC that controls the separator. The estimators use pre-inverted measurements to obtain a linear mapping between the states and measurements. The NMHE uses multiple shooting for transcribing the continuous-time optimization problem and an interior-point solver for solving the optimization problem.

The estimator performance was studied in two separate simulations for the same conditions. The estimation performance was evaluated based on the statistical properties of the estimates revealing better performance for the UKF than for the NMHE. The control and closed-loop system performance were evaluated based on RMS values of the control and closed-loop system error. The results showed that the MPC using state feedback from the UKF achieved slightly better level control, while the MPC using state feedback from the NMHE achieved slightly better pressure control. However, the differences between the estimators were relatively small and their performances are sensitive to tuning. Thus, a different tuning might change the result.

In the prediction model, the pressure dynamics is nonlinear and largely described by unknown parameters resulting in a poor prediction model. This relatively poor prediction model is likely to cause the larger oscillations in the pressure estimate compared to the other estimates experienced by both

The UKF is able to estimate the unknown parameters with negligible bias from the true values, while the NMHE experiences a small bias. The overall performance may be improved by compensating for this bias. Thus, bias estimation using a disturbance model is left as future work.

In reality, the level measurement in a GLCC separator is often unavailable and difficult to measure because of the complex, non-flat liquid surface. Therefore, estimation of the liquid level from other measurements is an unsolved problem left as future work.

ACKNOWLEDGMENTS

This project is supported by the Norwegian Research Council, industrial partners and NTNU under the Subsea Production and Processing (SUBPRO) SFI program.

REFERENCES

[1] O. T. McClimans and R. Fantoft, "Status and new development in subsea processing," in *Offshore Technology Conference*, 2006.

[2] G. E. Kouba, S. Wang, L. E. Gomez, R. S. Mohan, and O. Shoham, "Review of the state-of-the-art gas-liquid cylindrical cyclone (GLCC) technology-field applications," in *International Oil & Gas Conference and Exhibition in China*, 2006.

[3] O. Kristiansen, Ø. Sørensen, and O. R. Nilssen, "Compactsep– compact subsea gas-liquid separator for high-pressure wellstream boosting," in *Offshore Technology Conference*, 2016.

[4] A. Ulfnes, T. Frost, P. Rylandsholm, O. Endersen, S. Johnsen, and A. Hermansen, "Guidelines for design of cost efficient and robust sensor based environmental monitoring systems," in *Society of Petroleum Engineers*, 2016.

[5] T. A. Johansen and T. I. Fossen, "Nonlinear filtering with eXogenous Kalman Filter and Double Kalman Filter," in *Proceedings of the European Control Conference*, 2016.

[6] S. J. Julier and J. K. Uhlmann, "Unscented filtering and nonlinear estimation," *Proceedings of IEEE*, 2004.

[7] P. Kühl, M. Diehl, T. Kraus, J. P. Schlöder, and H. G. Bock, "A real-time algorithm for moving horizon state and parameter estimation," *Computers and Chemical Engineering*, 2011.

[8] T. T. Kristoffersen and C. Holden, "Model predictive control and extended Kalman filter for a gas-liquid cylindrical cyclone," in *Proceedings of the 1st IEEE Conference on Control Technology and Applications*, 2017.

[9] S. J. Ohrem, T. T. Kristoffersen, and C. Holden, "Adaptive feedback linearizing control of a gas-liquid cyclindrical cyclone," in *Proceedings of the 1st IEEE Conference on Control Technology and Applications*, 2017.

[10] T. T. Kristoffersen, C. Holden, and O. Egeland, "Feedback linearizing control of a gas-liquid cylindrical cyclone," in *Proceedings of the 20th World Congress of the Internation Federation of Automatic Control*, 2017.

[11] T. T. Kristoffersen and C. Holden, "State and parameter estimation of a gas-liquid cylindrical cyclone," in *Proceedings of the European Control Conference*, 2018.

[12] T. T. Kristoffersen, C. Holden, S. Skogestad, and O. Egeland, "Control-oriented modelling of a gas-liquid cylindrical cyclone," in *Proceedings of the American Control Conference*, 2017.

[13] T. T. Kristoffersen and C. Holden, "Nonlinear model predictive control of a gas-liquid cylindrical cyclone," in *Proceedings of the 25th Mediterranean Conference on Control and Automation*, 2017.

[14] J. M. Maciejowski, *Predictive Control with Constraints*. Pearson Education Limited, 2002.

[15] J. Andersson, J. Åkesson, and M. Diehl, "CasADi – a symbolic package for automatic differentiation and optimal control," in *Recent Advances in Algorithmic Differentiation*, 2012.

[16] A. C. Hindmarsh and R. Serban, *User documentation for CVODES v3.1.0*, nov 2017.

[17] A. Wächter and L. T. Biegler, "On the implementation of an interior-point filter line-search algorithm for large-scale nonlinear programming," in *Mathematical programming*, 2006.

[18] R. Kandepu, B. Foss, and L. Imsland, "Applying the unscented Kalman filter for nonlinear state estimation," *Journal of process control*, 2008.

[19] D. Simon, *Optimal state estimation*. Wiley, 2006.

[20] M. Diehl, J. Ferreau, and N. Haverbeke, "Efficient numerical methods for nonlinear MPC and moving horizon estimation," in *Nonlinear Model Predictive Control*. Springer-Verlang Berlin Heidelberg, 2009.